

# FDTD Study on Wave Propagation in Biaxial Anisotropic Metamaterials

Maoyan Wang<sup>1</sup>, Jian Wu<sup>2</sup>, Jun Xu<sup>1</sup>, Hailong Li<sup>3</sup>, Debiao Ge<sup>3</sup>

<sup>1</sup>School of Physical Electronics, University of Electronic Science and Technology of China, Chengdu, Sichuan 610054, China, wmybrimhl@163.com

<sup>2</sup>National Key Laboratory of Electromagnetic Environment, China Research Institute of Radiowave Propagation, Beijing 102206, China, Jian.Wu@263.net

<sup>3</sup> School of Science, Xidian University, Xi'an, Shanxi 710071, China, hailong703@163.com

## Abstract

Wave propagation in indefinite biaxial anisotropic metamaterials (AMM) is simulated with shift operator method in Finite-Difference Time-Domain method. The directions of wave vector and energy flow densities in AMM slabs affected by the relative permittivity and permeability tensors of AMM are analyzed. The potential applications of AMMs in cloak, beam splitter, solid-state spectroscopy, and omnidirectional linear polarizer are investigated.

## 1. Introduction

A medium with negative permittivity and permeability was introduced by Veselago in 1968 [1]. In 2001, inspired by the work of Pendry [2] *et al.*, Smith *et al.* foremost constructed a composite “medium” in the microwave regime by arranging periodic arrays of small metallic wires and split-ring resonators (SRRs) [3]. These kinds of media can also be mentioned metamaterials, negative-index materials *et al.*. Soon, Alternative realizations of metamaterials that consisted of host transmission lines with embedded lumped series capacitors and shunt inductors are proposed and realized [4]. The structures (interlacing wires and split-ring resonators) investigated in experiments are strongly anisotropic. Finite-Difference Time-Domain method (FDTD) can study not only metamaterial made of SRRs and metallic wires, but also metamaterial is equivalent to dispersive media [5]. For the latter case, the problem which incorporates both anisotropy and frequency dispersion at the same time can be solved for the anisotropic metamaterial (AMM) slabs by the shift operator (SO) method in FDTD. In the paper, SO-FDTD is briefly introduced. Wave propagation in four kinds of AMMs is simulated with SO-FDTD to discuss their applications.

## 2. FDTD Simulator

Here SO-FDTD is briefly introduced below. The Maxwell equations are

$$\nabla \times \mathbf{E} = -\partial \mathbf{B} / \partial t, \quad \nabla \times \mathbf{H} = \partial \mathbf{D} / \partial t \quad (1)$$

In the frequency domain, the constitute relation of an AMM and Drude models can be described as

$$\mathbf{D} = \varepsilon_0 \begin{bmatrix} \varepsilon_x & 0 & 0 \\ 0 & \varepsilon_y & 0 \\ 0 & 0 & \varepsilon_z \end{bmatrix} \mathbf{E}, \quad \mathbf{B} = \mu_0 \begin{bmatrix} \mu_x & 0 & 0 \\ 0 & \mu_y & 0 \\ 0 & 0 & \mu_z \end{bmatrix} \mathbf{H}, \quad \begin{aligned} \varepsilon_i &= 1 - \omega_{pe}^2 / [\omega(\omega + i\Gamma_e)] \\ \mu_i &= 1 - \omega_{pm}^2 / [\omega(\omega + i\Gamma_m)] \end{aligned} \quad (2)$$

For TE wave case, Equation (1) and (2) are discretized by using Yee's scheme, only  $B_x$  and  $H_x$  are given

$$\begin{aligned} B_x^{n+1/2}(i, k+1/2) &= B_x^{n-1/2}(i, k+1/2) + \Delta t \left[ (E_y^n(i, k+1) - E_y^n(i, k)) / \Delta z \right] \\ H_x^{n+1/2} &= \left[ (a_0 B_x^{n+1/2} + a_1 B_x^{n-1/2} + a_2 B_x^{n-3/2}) / \mu_0 - b_1 H_x^{n-1/2} - b_2 H_x^{n-3/2} \right] / b_0 \\ a_0 &= q_0 + 2q_1 / \Delta t + q_2 (2/\Delta t)^2 \quad a_1 = 2q_0 - 2q_2 (2/\Delta t)^2 \quad a_2 = q_0 - 2q_1 / \Delta t + q_2 (2/\Delta t)^2 \quad p_0 = \omega_{pm}^2 \quad p_1 = \Gamma_m \quad p_2 = 1 \\ b_0 &= p_0 + 2p_1 / \Delta t + p_2 (2/\Delta t)^2 \quad b_1 = 2p_0 - 2p_2 (2/\Delta t)^2 \quad b_2 = p_0 - 2p_1 / \Delta t + p_2 (2/\Delta t)^2 \quad q_0 = 0 \quad q_1 = \Gamma_m \quad q_2 = 1 \end{aligned} \quad (3)$$

### 3. FDTD Numerical Results and Discussion

As shown in reference [6], indefinite AMMs are identified as four classes of media based on their cutoff properties of wave vector  $q_x$ . Each type of the AMMs has two subtypes. Table 1 gives the classification of the four types of AMMs. In Table 1,  $\theta$  is incident angle and  $\theta_c$  is critical angle separating propagating from evanescent solutions. The propagation conditions are also given in Table 1. Total reflection occurs for Always Cutoff media at any angle and for Cutoff media if incident angle  $\theta > \theta_c$  or for Anti-Cutoff media if  $\theta < \theta_c$ .

Table 1 the classification of four types of anisotropic metamaterials

Type	Cutoff	Never Cutoff	Anti-Cutoff	Always Cutoff
Media condition	$\epsilon_y \mu_x > 0 \quad \mu_x / \mu_z > 0$	$\epsilon_y \mu_x > 0 \quad \mu_x / \mu_z < 0$	$\epsilon_y \mu_x < 0 \quad \mu_x / \mu_z < 0$	$\epsilon_y \mu_x < 0 \quad \mu_x / \mu_z > 0$
Propagation	$\theta < \theta_c$	Any $\theta$	$\theta > \theta_c$	No real $q_x$

The interactions between TE-polarized wave and four kinds of AMMs are simulated with SO-FDTD in this section. The 2D FDTD simulator solves the equivalent TE wave set for  $E_y$ ,  $H_x$  and  $H_z$ . The cell sizes are  $\Delta x = \Delta z = 0.02\text{cm}$  long. The time step is set to be  $\Delta t = \Delta z / 2c$ . Except for Cutoff media case, the Gaussian beam  $s(t) = \sin(\omega_0 t)$  is launched into the total field region using a total-scattered field (TF-SF) formulation. The CW frequency is chosen to be  $f_0 = 30\text{GHz}$ . The focal plane of the beam is taken to be the TF-SF boundary. The beam varies spatially as  $\exp(-x^2/w_0^2)$  on that boundary with its waist  $w_0 = 50\Delta z$ . AMM slabs below are outlined with solid line.

#### 3.1 Cutoff Media Case

Figure 1 shows the interaction between TE-polarized wave and three kinds of five parallel cylinders array placed symmetry around the  $y$ -axis with center of all cylinders located on the  $x$ -axis. The frequency of the incident wave is 10GHz. The radius of the cylinder is  $0.1\lambda_0$  and the distance between the centers of the cylinders is  $0.5\lambda_0$ . As shown in Fig. 1(a), the backward scattering of metallic cylinders is large whereas the forward scattering is small. The material parameters of Subtype I of Cutoff media cylinders in Fig. 1(b) are  $\mu_x = \mu_z = \epsilon_y = -5$ . The result shows a great focusing of the field in the forward direction. In Fig. 1(c), every metallic cylinder with  $0.1\lambda_0$  radius is coated with Cutoff media layer of thickness  $0.05\lambda_0$  and  $\mu_x = \mu_z = \epsilon_y = -5$ . By comparing Fig. 1(a) and Fig. 1(c), Cut off media make the backward scattering of metallic cylinders decrease and forward scattering increase.

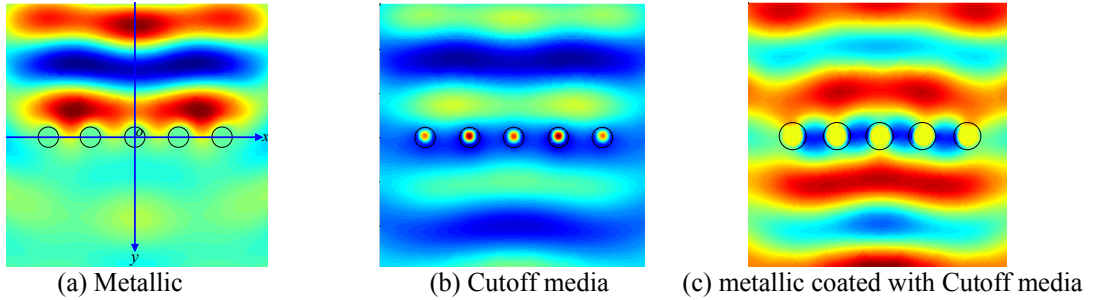


Figure 1. FDTD predicts the near field distribution of three kinds of five parallel cylinders array,  $t=6000\Delta t$ .

#### 3.2 Never Cutoff Media Case

In Fig. 2 (c),  $\mathbf{q}$  and  $\mathbf{v}_g$  specifies the directions of wave vector and energy flow density  $\mathbf{S}$  in Never Cutoff media slabs. The directions of  $\mathbf{q}$  and  $\mathbf{v}_g$  are no longer parallel or antiparallel like isotropic medium. The energy flow density  $\mathbf{S}$  in AMM is

$$\mathbf{S} = \text{Re} \left[ \frac{T_{\text{TE}}^2 E_0^2 q_x}{2\omega \mu_0 \mu_z} \hat{x} + \frac{T_{\text{TE}}^2 E_0^2 q_z}{2\omega \mu_0 \mu_x} \hat{z} \right] \quad (4)$$

Figure 2 gives electric field intensity distributions for slabs of two subtypes of Never Cutoff media embedded in free space and dispersion plot for Never Cutoff media. As shown in Fig. 2 (a), (c),  $q_z$  is negative and anomalous refractions occur in subtype I of Never Cutoff media, whereas the energy flow is positively refracted in subtype I of Never Cutoff media slab. In Fig. 2 (b), (c),  $q_z$  is positive and regular refractions occur in subtype II of Never Cutoff media, though the shift of Gaussian beam propagating through the AMM slab is negative. Because the transverse component of the wave vector,  $q_x$ , is conserved across the interface according to the boundary conditions, and causality requires that in the second medium, energy flow of the refracted waves should be transmitted away from the interface of the two media but never toward the interface [6]. The  $q_x > 0$  and  $v_{gz} > 0$  ( $S_z > 0$ ) sketched in Fig.2 agree with the above two rules. As one can see in Eq. (4),  $q_z$  and  $\mu_x$  must have the same signs because of  $S_z > 0$ ,  $S_x$  and  $\mu_z$  must have the same signs because of  $q_x > 0$ . A compact and very efficient beam splitter based on large birefringence can be made of AMM to route wave, if one polarized wave is positively refracted ( $v_{gx} > 0$ ) whereas the other is negatively refracted ( $v_{gx} < 0$ ). The AMM slab can be realized with ring and rod.

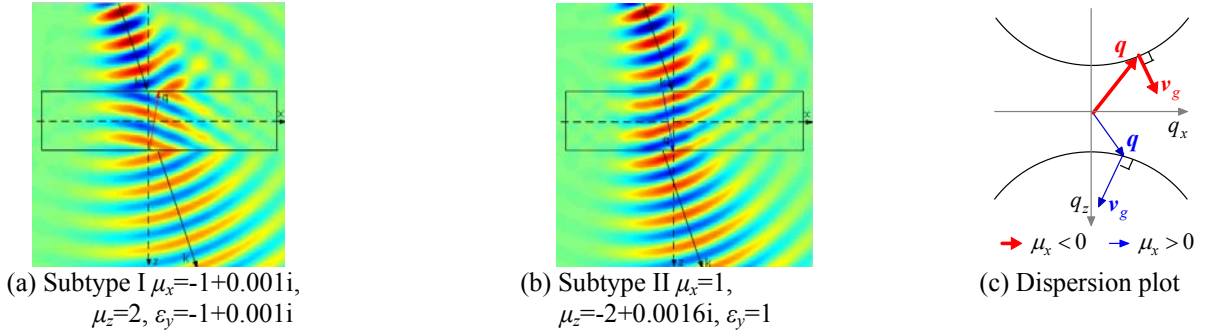


Figure 2. FDTD predicts electric field intensity distributions for the interaction of the Gaussian beam that is incident at  $20^\circ$  and  $t=7500\Delta t$  to two subtypes of Never Cutoff media slabs and dispersion plot.

### 3.3 Anti-Cutoff Media Case

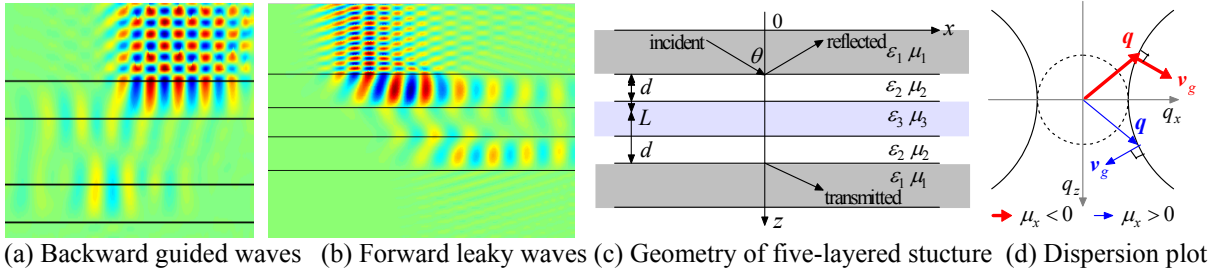


Figure 3. FDTD predicts field intensity distributions for Gaussian beam propagation in five-layered structures with  $\varepsilon_1 = 12.8$ ,  $\mu_1 = \varepsilon_2 = \mu_2 = 1$  and the third media, i.e. Anti-Cutoff media (a) subtype II having  $\varepsilon_y = -2$ ,  $\mu_x = 0.2$ ,  $\mu_z = -0.2$ ,  $d = 0.5\lambda_0$ ,  $L = 0.8\lambda_0$ ,  $t = 4000\Delta t$ ,  $\theta = 75^\circ$ , (b) subtype I having  $\varepsilon_y = 2$ ,  $\mu_x = -0.2$ ,  $\mu_z = 0.2$ ,  $d = \lambda_0$ ,  $L = 0.8\lambda_0$ ,  $t = 2800\Delta t$ ,  $\theta = 70^\circ$ , (c) Geometry of five-layered structure, (d) dispersion plot.

Figure 3 shows the Gaussian beam propagation in five-layered structures that include two subtypes of Anti-Cutoff media and dispersion plot for Anti-Cutoff media. Backward guided waves are excited at the boundary between air and subtype II of Anti-Cutoff media. The conditions for the excitation of the backward surface waves if the third medium is anisotropic medium is not restricted by those if the third medium is isotropic metamaterial. Because  $\mu_z < 0$ , the energy flow density is negatively refracted, even if the wave vector is forward. The amplitude of the backward guided wave is lower than the incident wave. The forward guided waves can be treated as excitations of leaky waves that are guided by the air gaps.

### 3.4 Always Cutoff Media Case

Due to Total reflection always occurs when the beam incident from isotropic medium to Always Cutoff media slabs at any angle. Figure 4 presents FDTD predicting the electric intensity distributions for the interaction between Gaussian beam and two types of Always Cutoff media slabs. Positive or negative Goos-Hänchen shift phenomena occur. To every kind of electric field, the sign of Goos-Hänchen shift for the two types of Always Cutoff AMM are opposite. However for Never Cutoff media, total reflection phenomena never

occurs at any incident angle. Omnidirectional linear polarizer can be realized by AMM slab, if one polarized wave is omnidirectional total transmission whereas the other is omnidirectional total reflection. According to the principle of duality, the interactions between TM-polarized wave and four kinds of AMMs can also be simulated with SO-FDTD.

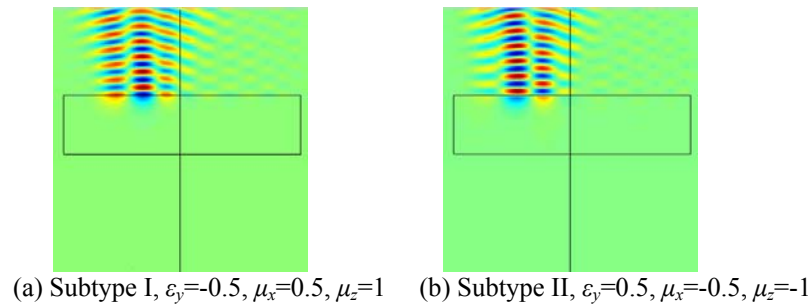


Figure 4. FDTD predicts electric field intensity distributions for the Gaussian beam that is incident at  $30^\circ$  from isotropic media with  $\mu_1=\varepsilon_1=2, \varepsilon_3=\mu_3=1$  to an Always Cutoff AMM slabs,  $d=2\lambda_0, t=7500\Delta t$ .

#### 4. Conclusion

In conclusion, the shift operator method in FDTD is briefly derived. The interaction between electromagnetic wave and four kinds of AMMs is simulated with SO-FDTD. Due to their anomalous characteristics, such as negative refraction, total reflection, and total transmission *et al.*, AMMs has potential applications in cloak, beam splitter, solid-state spectroscopy, and omnidirectional linear polarizer *et al.* Nonetheless, their eventual usefulness for the potential practical applications will depend greatly on clever fabrication concepts and implementations in those scenarios.

#### 5. Acknowledgments

This work was supported by National Key Laboratory of Electromagnetic Environment fund under Grant No.51486030305HT0101 and 9140C08060507ZCZJ18.

#### 6. References

1. V. G. Veselago, "The electrodynamics of substances with simultaneously negative values of  $\varepsilon$  and  $\mu$ ," *Sov. Phys. Usp.*, 1968, Vol. 10, No. 4, pp. 509-514.
2. J. B. Pendry, A. J. Holden, D. J. Robbins, and W. J. Stewart, "Magnetism from conductors and enhanced nonlinear phenomena," *IEEE Trans. Microwave Theory Tech.*, 1999, Vol. 47, No. 11, pp. 2075-2084.
3. R. A. Shelby, D. R. Smith, and S. Schultz, "Experimental verification of a negative index of refraction," *Science*, 2001, Vol. 292, No. 6, 77-79.
4. A. Lai, C. Caloz, T. Itoh, "Composite right / left-handed transmission line metamaterials," *IEEE Microwave Magazine*, 2004, 35-50.
5. R. W. Ziolkowski, "Pulsed and CW Gaussian beam interactions with double negative metamaterial slabs," *Optics Express*, 2003, Vol. 11, No. 7, 662-681.
6. D. R. Smith, and D. Schurig, "Electromagnetic wave Propagation in media with indefinite permittivity and permeability tensors," *Physical Review Letters*, 2003, Vol. 90, No. 7, 077405, 1-5.